Cold Regions Science and Technology 74–75 (2012) 31–42

Contents lists available at SciVerse ScienceDirect

Cold Regions Science and Technology

journal homepage: www.elsevier.com/locate/coldregions

# How much of the real avalanche activity can be captured with tree rings? An evaluation of classic dendrogeomorphic approaches and comparison with historical archives

Christophe Corona [a,b,*], Jérôme Lopez Saez [a], Markus Stoffel [b,c], Mylène Bonnefoy [d], Didier Richard [c], Laurent Astrade [e], Frédéric Berger [a]

[a] Cemagref UR EMGR, 2 rue de la Papeterie, BP 76, F 38402 St-Martin-d'Hères cedex, France
[b] Laboratory of Dendrogeomorphology (dendrolab.ch), Institute of Geological Sciences, University of Berne, Baltzerstrasse 1 + 3, CH-3012 Berne, Switzerland
[c] Climatic Change and Climate Impacts, Institute for Environmental Sciences, University of Geneva, 7 Route de Drize, CH-1227 Carouge, Switzerland
[d] Cemagref UR ETNA, 2 rue de la Papeterie, BP 76, F-38402 St-Martin-d'Hères cedex, France
[e] Université de Savoie, CISM, Laboratoire EDYTEM, Bâtiment Belledonne, Campus de Technolac, F-73370 Le Bourget du Lac, France

ARTICLE INFO

*Article history:*
Received 27 August 2011
Accepted 9 January 2012

*Keywords:*
Dendrogeomorphology
Historical archives
Snow avalanches
Spatio-temporal analysis
French Alps

ABSTRACT

In snow-rich areas, snow avalanches endanger settlements and cause heavy damage to infrastructure or transportation routes. In wooded avalanche paths, dendrogeomorphology has been used extensively to reconstruct snow avalanche histories or to complement existing archival records. Several authors noted (i) that avalanche chronologies reconstructed from tree rings would depend on the number of trees sampled, and on (ii) the minimum number of tree-ring responses; and (iii) that they would always represent minimum frequencies. These restrictions gave rise to the question of how much of the real avalanche activity can be captured in tree-ring records. We therefore performed a dendrogeomorphic analysis based on 175 *Larix decidua* Mill. and 34 *Picea abies* (L.) Karst. trees from an extensively and accurately documented (1905–2010) avalanche path located in the Arve valley (French Alps) to obtain optimal thresholds for sample size and index values (i.e. percentage of responses in relation to the number of trees alive for a given year). Results clearly demonstrate that a sample size of ~100 trees is needed to obtain the best match between reconstruction (tree rings) and documentation (archives) while minimizing the inclusion of noise in the dendrogeomorphic record. Validation of the reconstruction (1771–2010) with historical archives shows that 13 undocumented events could be added to the archival record and that 43% of all documented events were deciphered with dendrogeomorphic techniques. The reconstruction of the spatial extent and reach of past snow avalanches matches with historical archives as far as the longitudinal extent of the largest avalanches is concerned. Yet, tree-ring records tend to underestimate runout elevations for a majority of minor events. Large discrepancies are also reported between the lateral limits derived with dendrogeomorphic techniques and the data reported in historical reports and hazard maps, with tree-ring data suggesting larger lateral spread of avalanche snow.



## 1. Introduction

Snow avalanches are major hazards to humans living in or visiting mountain ranges around the world. Densely populated mountain regions have experienced the largest amount of avalanche-related death tolls and infrastructural damage over the centuries. In the Alps, for example, the earliest chronologies date back to the 14th century (Casteller et al., 2011). These archival records have repeatedly been used in the past to document the chronology and the extent of past avalanches. Other empirical methods used by practicioners included terrain analysis (e.g., change analysis in time series of aerial photographs, vegetation studies) and/or interviews with (elderly) residents. Although these approaches represent an indispensible step in avalanche hazard assessments (Ancey, 2004), (i) they strongly rely on the experience of a few individuals and inevitably suffer from shortcomings: archival records of past avalanche events do not normally yield data with satisfying spatial and temporal resolution or (ii) precision (e.g., runout distance, avalanche type). In addition, historic documentation is most often (iii) biased toward events that caused damage to structure or loss of life on one hand and (iv) nonexistent in unpopulated areas on the other hand (Bollschweiler et al., 2011).

Where avalanche paths are covered with forest, dendrogeomorphology can be used to date past avalanche events with annual resolution and for periods covering the past decades to centuries (Butler and Sawyer, 2008). The basic principles of tree-ring dating of mass-

* Corresponding author at: Cemagref UR EMGR, 2 rue de la Papeterie, BP 76, F 38402 St-Martin-d'Hères cedex, France. Tel.: +33 476762784.
*E-mail address:* christophe.corona@cemagref.fr (C. Corona).

0165-232X/$ – see front matter © 2012 Elsevier B.V. All rights reserved.
doi:10.1016/j.coldregions.2012.01.003

movement processes have been outlined e.g., by Alestalo (1971), Butler (1987), Stoffel and Bollschweiler (2008) and Stoffel et al. (2010a). Dendrogeomorphology is based on the fact that trees form one increment ring per year in temperate climates and that trees affected by geomorphic processes will record the event in the form of characteristic growth disturbances (GD) in their tree-ring series. The use of tree rings for the reconstruction of chronologies of snow avalanching has a decades-long history, with increasing sophistication characterizing most recent applications (Butler and Sawyer, 2008). Pioneering dendrogeomorphic studies on snow avalanches date back to the 1960s when Potter (1969) and Schaerer (1972) developed the first avalanche reconstructions in North America (also see Table 1 and Butler and Sawyer (2008) for a recent review). Dendrogeomorphic analyses of snow avalanches were unusual in Europe before the early 2000s but were becoming increasingly popular in the early 2000s (Table 1), particularly in the Alps (e.g., Casteller et al., 2007; Corona et al., 2010; Stoffel et al., 2006) and Pyrenees (Muntán et al., 2009).

It has been noted in previous work that avalanche histories derived from tree-ring records would always remain incomplete (Reardon et al., 2008) and that the resulting time series would therefore represent minimum frequencies of past activity (Stoffel et al., 2006). Past events may have been missed as a result of tree selection in the field or through the fact that avalanches did not leave any signs in the trees currently present in the avalanche path (Stoffel et al., 2010b). Previous dendrogeomorphic work on snow avalanches also suffered from the lack of a uniform agreement concerning minimum sample size (i.e. sample size) and the minimum number (and intensity) of growth disturbances (GD) necessary for the recognition of a past avalanche event (Butler and Sawyer, 2008; Butler et al., 1987; Germain et al., 2009).

As a consequence, these restrictions give rise to the question of how much of the real avalanche activity can be captured in the tree-ring series. While it is true that past dendrogeomorphic reconstructions have been compared with (limited) archival records (e.g., Corona et al., 2010; Dubé et al., 2004; Hebertson and Jenkins, 2003; Reardon et al., 2008), snow avalanche histories derived from tree-ring records have not been calibrated on consistently and systematically documented paths so far.

It was therefore the purpose of this study to (i) compile archival data for an unusually well-documented avalanche path in the French Alps; (ii) illustrate how variations in the minimum number of responding samples can result in variations in snow avalanche chronologies; (iii) quantify the proportion and nature of snow avalanches reconstructed with dendrogeomorphic techniques; and to (iv) evaluate the spatial reliability and accuracy of tree-ring reconstructions.

## 2. Study site

The present study was conducted on the north-facing slope of the Arve Valley in the Northern French Alps (Haute-Savoie, 45°54′N, 6°51′E, Fig. 1), where the Pèlerins avalanche path extends from 1100 to 3650 m asl and dominates the hamlet of Les Pèlerins, located 2 km southwest of downtown Chamonix. Snow avalanches are commonly naturally triggered from a starting zone (50 ha) located between 2750 and 3650 m asl (mean slope angle: 36°) where an orthogneissic rockwall is partly covered by the Pèlerins glacier. Once released, snow avalanches pass through a conical track (mean slope angle: 30°, path length: 1200 m) before reaching the runout zone (15 ha) at 1350 m asl.

A characteristic transverse vegetation pattern (Malanson and Butler, 1984) can be observed across the track: The inner zone is colonized by dense shrubs and shade-intolerant pioneer tree species with flexible stems, such as green alder (*Alnus viridis* (Chaix) DC), European rowan (*Sorbus aucuparia* L.) and silver birch (*Betula pendula* Roth.). In the outer zone, European larch (*Larix decidua* Mill.) and Norway spruce (*Picea abies* (L.) Karst.) are dominant. Located in the upper mountain stage (Ozenda, 1985), the runout zone is covered by a dense forest dominated by *P. abies*. A vast majority of trees around the track and within the runout zone exhibit clear signs of disturbance from multiple avalanche events.

According data from the nearby meteorological station of Chamonix (1054 m asl), annual temperature is 6.6 °C for the 1935–1990 period and annual precipitation amounts to 1262 mm for the 1934–1990 period (Zumbühl et al., 2008). For the same periods, winter temperature (DJF) is −2.5 °C and winter precipitation amounts to 311 mm (Zumbühl et al., 2008). Between December and April, precipitation falls primarily as snow. Average annual snowfall reaches 287 cm (±121 cm) for the period 1960–2007.

The Pèlerins avalanche path threatens the hamlet of Les Pèlerins and the first section of the Aiguille du Midi cable car (Les Pèlerins-La Para), which has been constructed for the first Winter Olympics in 1924. In addition, the access road to the Mont Blanc Tunnel crosses the runout zone several times below 1275 m asl. This tunnel is a major north–south connection for Europe and two million vehicles have been counted on this road per year, of which 33% are trucks (Deline, 2009). As a result of the intense and multi-purpose use of the area, abundant and continuous historical records are available for the Pèlerins avalanche path.

## 3. Materials and methods

### 3.1. Compilation of historical archives

Several documentary sources were used in this study to compile a precise and as complete as possible historical chronology of avalanche events in the Pèlerins path. Most of the recent data were extracted from the "Enquête Permanente des Avalanches" (EPA), a chronicle describing the history of avalanche events for ~5000 recognized paths in the French Alps and the Pyrenees (Eckert et al., 2009). These EPA records are usually complemented with a map (Carte de Localisation des Phénomènes Avalancheux; hereafter referred to as CLPA) localizing the release zones, lateral extent, runout elevations, and type of snow avalanches (Jamard et al., 2002). As a result of the potential threat to infrastructure, the Pèlerins avalanche path has received considerable attention in the past and activity has been documented continuously and with unusual accuracy since the beginning of the 20th century. In addition, technical reports (e.g., ETNA, 2000; Lagotala, 1927; Leone, 2006), aerial photographs and terrestrial photographs were used to assess the extent of high-magnitude events.

Data on pre-20th century events were derived from diaries, paintings and municipal archives (Lambert, 2009). Particularly, the events for the period 1779–1802, 1830–1850 and 1860–1881 were derived from diaries written by J.M. Cachat (Cachat, 2000), F.X. Cachat and J.A. Couttet (Chaubet, 2011; Leone, 2006) and F. Savioz (Leone, 2006), respectively.

### 3.2. Dendrogeomorphic analysis

The reactions of trees to snow avalanches are driven by the forces of the avalanche and the mechanical impact of debris (i.e. rocks and boulder or broken trees) transported by the snow as well as by the size and flexibility of the tree itself (Bebi et al., 2009). Typical morphologies of avalanche trees include tilting, wounding as well as trunk, apex and branch breakage (Bartelt and Stöckli, 2001; Luckman, 2010). These external anomalies are reflected in the wood with anomalous anatomical features, which can be detected and accurately dated in tree-ring series using dendrogeomorphic techniques (e.g., Stoffel and Bollschweiler, 2008, 2009). The reactions most commonly observed in tree rings following avalanche activity are (i) a distinct growth suppression (Butler and Malanson, 1985) following apex loss or the break-off of branches (Johnson, 1987), (ii) the formation of compression wood (Timell, 1986) with thicker (rounder) and slightly darker tracheids (Stoffel and Bollschweiler, 2008) after tilting and (iii) the production of chaotic callus tissue (Stoffel et al., 2010a) and tangential rows of

traumatic resin ducts (referred hereafter as to TRD) at the edges of the injury after wound infliction and/or cambium damage (Schneuwly et al., 2008; Stoffel and Hitz, 2008).

For this investigation, we used the appearance of callus tissue and TRD, the initiation of compression wood and abrupt growth reductions to determine the occurrence of avalanches. A total of 209 trees (175 *L. decidua* and 34 *P. abies* trees) damaged by snow avalanches was sampled with 452 increment cores. A minimum of two increment cores were extracted per tree, with one from upslope in the assumed direction of past avalanche event and one in the opposite direction. GPS coordinates were recorded for each tree with 1-m accuracy using a Trimble GeoExplorer. For each tree, additional data were collected including

**Table 1**
Bibliographic synthesis on tree-ring reconstructions of snow avalanches.

| Authors | Year | Country | Location | Number of paths | Species | Sample depth | Period | Number of growth disturbances | Minimal Index value | Number of avalanche events |
|---|---|---|---|---|---|---|---|---|---|---|
| Potter | 1969 | USA | Wyoming | | | 17 | | | | |
| Schaerer | 1972 | Canada | British Columbia | Unknown | Unknown | Unknown | Unknown | Unknown | Unknown | Unknown |
| Smith | 1973 | USA | Washington | 13 | Unknown | Unknown | Unknown | Unknown | Unknown | Unknown |
| Ives et al. | 1976 | USA | Colorado | Unknown | *Populus tremuloides, Picea engelmannii* | Unknown | 1860–1974 | 56 | Unknown | 6 |
| Carrara | 1979 | USA | Colorado | 1 | *Populus tremuloides, Picea engelmannii, Abies lasiocarpa,* | 50 | 1880-1976 | Unknown | Unknown | 4 |
| Butler | 1979 | USA | Montana | 5 | | 30 | | | | |
| Butler and Malanson | 1985 | USA | Montana | 2 | *Picea engelmannii, Abies lasiocarpa, Pseudotsuga menziesii, Larix occidentalis, Pinus contorta* | 30 + 48 | 1924-1979 1934-1981 | Unknown | 40% | 10 + 15 |
| Frazer | 1985 | Canada | Alberta | | | | | | | |
| Johnson et al. | 1985 | Canada | Alberta | | | | | | | |
| Bryant et al. | 1989 | USA | Colorado | 3 | *Populus tremuloides, Picea engelmannii* | 60 + 60 + 60 | Unknown | Unknown | Unknown | Unknown |
| Patten and Knight | 1994 | USA | Wyoming | | | | | | | |
| Rayback | 1998 | USA | Colorado | 2 | | | | | | |
| Larocque et al. | 2001 | Canada | Québec | 1 | *Picea glauca, Picea mariana, Abies balsamea, Larix laricina* | 111 | 1885–2000 | Unknown | 10% | 3 |
| Hebertson and Jenkins | 2003 | USA | Utah | 16 | *Picea engelmannii, ,Abies lasiocarpa,* | 297 (8–26) | 1928–1996 | Unknown | Unknown | 14 |
| Boucher et al. | 2003 | Canada | Québec | 1 | *Abies balsamea, Picea mariana* | 62 | 1895–1996 | Unknown | 10% | 35 |
| Jenkins and Hebertson | 2004 | USA | Utah | 1 | *Picea engelmannii, Abies concolor, Populus tremuloides* | 78 | 1891–1995 | Unknown | Unknown | 13 |
| Dubé et al. | 2004 | Canada | Québec | 3 | *Thuya occidentalis, Abies balsamea, Betula papyrifera.* | 62 + 20 + 28 | 1871–1996 | Unknown | 10% | 7 |
| Muntan et al. | 2004 | Spain | Pyrenees | 1 | *Pinus uncinata* | 230 | 1750–2000 | Unknown | Unknown | 3 |
| Kajimoto et al. | 2004 | Japan | | 1 | *Abies mariesii* | 34 | Unknown | Unknown | Not computed | Not computed |
| Germain et al. | 2005 | Canada | Québec | 2 | Unknown | 78 + 52 | 1941–2004 | 420 | Unknown | 11 |
| Pederson et al. | 2006 | USA | Montana | 1 | *Pseudotsuga menziesii* | 109 | 1910–2003 | Unknown | 10% | 27 |
| Stoffel et al. | 2006 | Switzerland | Alps | 1 | *Larix decidua* | 251 | 1750–2002 | 561 | Unknown | 9 |
| Casteller et al. | 2007 | Switzerland | Alps | 2 | *Larix decidua, Picea abies* | 66 + 79 | Unknown | Unknown | Not computed | Not computed |
| Mundo et al. | 2007 | Argentina | Andes | 1 | *Nothofagus pumilio* | 20 | Unknown | Unknown | Not computed | Not computed |
| Butler and Sawyer | 2008 | USA | Colorado | 2 | *Abies lasiocarpa, Pseudotsuga menziesii, Pinus contorta* | 10 + 12 | 1945–2008 1963–2008 | Unknown | 20%, 40% | 15 + 9 |
| Reardon et al. | 2008 | USA | Montana | 1 | *Pseudotsuga menziesii* | 109 | 1910–2003 | Unknown | 10% | 27 |
| Germain et al. | 2008 | Canada | Québec | 12 | Unknown | 10–243 | 1895–1999 | 51–799 | 10% | 19 |
| Laxton and Smith | 2008 | India | Himalaya | 1 | *Cedrus deodara* | 36 | 1972–2006 | Unknown | Unknown | 4 |
| Casteller et al. | 2008 | Argentina | Andes | 1 | *Nothofagus pumilio* | 50 | Unknown | Unknown | Unknown | 6 |
| Muntan et al. | 2009 | Spain | Pyrenees | 6 | *Pinus uncinata* | 26–131 | 1870–2000 | Unknown | 16–40% | 3 |
| Corona et al. | 2010 | France | Alps | 1 | *Larix decidua* | 232 | 1919–1994 | 901 | 10 | 20 |
| Köse et al. | 2010 | Turkey | Kayaarka | 2 | *Abies bornmuelleriana* | 61 | Unknown | Unknown | Not computed | Not computed |
| Casteller et al. | 2011 | Argentina | Andes | 9 | *Nothofagus pumilio* | 6-15 | 1820–2005 | Unknown | Unknown | 6 |

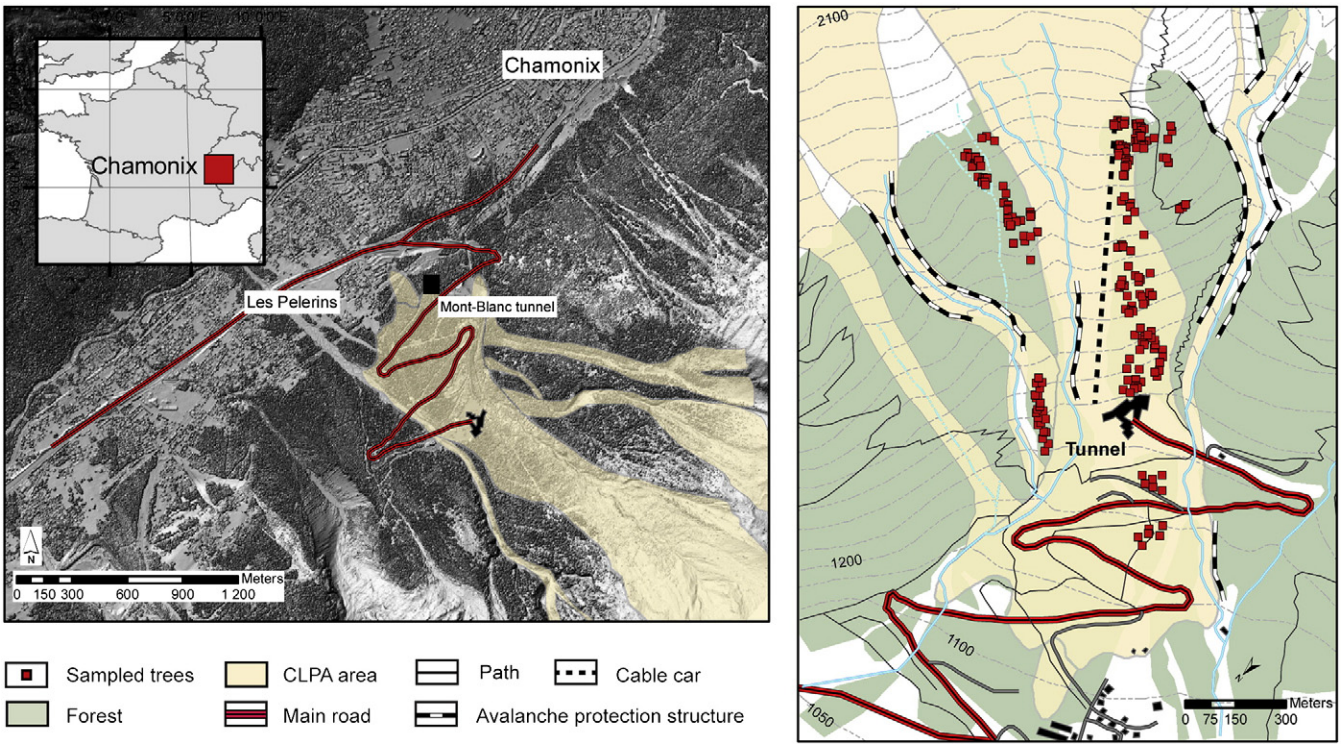


**Fig. 1.** The Arve Valley and the Pèlerins avalanche path.

its position within the avalanche track, its diameter at breast height (DBH), description of the disturbance (i.e. amount of impact scars, branch flagging, and tilting) and information on neighboring trees. Sampling height was chosen according to the morphology of the stem: (i) injured or tilted trees were sampled at the height of the disturbance; (ii) cross-sections and cores from decapitated trees were, in contrast, extracted next to the stem base so as to preserve as much tree-ring information as possible (Stoffel and Bollschweiler, 2008).

In addition to the disturbed trees sampled in the path, (iii) 24 undisturbed *L. decidua* trees showing no signs of avalanche activity or any other geomorphic process were selected outside of the active avalanche zone. Three cores were extracted per tree, two perpendicular to the slope and one in the downslope direction. The preparation and analysis of samples followed standardized geomorphic procedures as described in Stoffel and Bollschweiler (2008). Ring-width measurements were made with a digital LINTAB positioning table with an adjoining Leica stereomicroscope and the time-series analysis software TSAP (Rinntech, 2009). To detect dating errors (i.e. missing or false rings) the cross-dating quality was evaluated using the program COFECHA (Holmes, 1983) and the graphical function of the program TSAP. Resulting measurements were graphically and statistically compared with the reference chronology computed from undisturbed trees; missing or false rings were corrected where necessary. For samples heavily impacted by multiple avalanches, "marker years" recorded in neighboring trees were used to ensure accurate calendar dating (Reardon et al., 2008). Thereafter, all samples were visually inspected under a stereomicroscope to identify GD associated with geomorphic disturbances, including abrupt growth suppression, compression wood, injuries and TRD.

### 3.3. Tree-ring reconstruction of avalanches

In a subsequent step, we assigned scores to each avalanche-related GD using an approach similar to those used previously by Dubé et al. (2004), Reardon et al. (2008) or Corona et al. (2010):

- Intensity 5: Abrupt change in radial growth associated with stem breakage; or clear impact scar associated with obvious compression wood or TRD or growth suppression.
- Intensity 4: Clear scar, but no compression wood or suppression of growth or obvious compression wood that lasts for approximately three years.
- Intensity 3: Obvious compression wood during 1 or 2 successive growth years following the disturbance.
- Intensity 2: Compression wood or growth suppression present but not well defined; or compression wood present but formed when tree was young and more susceptible to damage from various environmental and biological factors.
- Intensity 1: Same as intensity 2 except that compression wood is very poorly defined, and slow onset may indicate other processes such as soil or snow creep as the primary causes of disturbance.

This rating system emphasizes features that are clearly associated with avalanche activity and discriminates against disturbances which can be induced by a variety of factors other than snow avalanches (e.g., improved light conditions or creeping snow). GD data from individual trees were then summarized in event response histograms (Dubé et al., 2004; Reardon et al., 2008; Shroder, 1980). For each year $t$, an index $I$ was calculated based on the percentage of trees showing responses ($R$) in their tree-ring record in relation to the number of trees sampled ($A$) being alive in year $t$:

$$It = \left(\left(\sum_{i=1}^{n} Rt\right) / \left(\sum_{i=1}^{n} At\right)\right) * 100$$

In our attempt to define acceptable minimum sample size and minimum numbers of responsive trees, we surveyed papers in which tree-ring analysis was utilized to reconstruct avalanche chronologies (Table 1). As no standard thresholds exist for a minimum number of trees responding to avalanche disturbance in a path, we defined optimal values for GD and *It* such that (i) the match between avalanches documented in archival records and those reconstructed

in the tree-ring series was maximized and (ii) noise in the tree-ring record was not considered an avalanche in case no event was recorded in the EPA. Definition of optimal values was limited to the accurately and continuously documented period 1905–2010. As optimal thresholds vary according to sample size (Butler and Sawyer, 2008), we extracted subsets of the entire sample with sample sizes varying from 10 to 200. To reduce the dependence on the sampling itself, and thus prevent addition of further noise to the reconstruction, 1000 subsets of $n$ trees, extracted without replacement, were computed for each sample size $n$ (with $n$ varying between 10 and 200).

For each subset, the total number of GD and *It* was computed for each year. Chronologies of reconstructed events were obtained by applying thresholds going from 2 to 10 for the minimum number of GD and from 1% to 50% for *It*. An avalanche year is determined in case both thresholds (for GD and *It*) are exceeded. These chronologies were then compared with historical archives. Reconstructed events which were absent from the archive were classified as noise. Final results are presented in the form of matrices and summarize the mean percentage of reconstructed events documented in historical archives and the mean number of events classified as noise according to the *It* and GD thresholds and based on 1000 sampling iterations.

## 4. Results

### 4.1. Historical avalanche chronology

Analysis of historical archives yielded data on 48 snow avalanche events at Pèlerins between 1776 and 2002, with a large majority of events (37) recorded during the 20th century (Fig. 2). The moderate mean avalanche frequency of 0.02 events $yr^{-1}$ for the period 1776–1900 certainly reflects discontinuity in the record and archives invariably emphasized avalanches which caused victims and/or damage to human structure. For example, the snow avalanche of 1779 was mentioned in historical archives most probably because it reached the hamlet of Les Bots. Similarly, in 1796 and 1818, avalanches killed four persons crossing the path. For the pre-20th century, temporary increases in avalanche frequency clearly reflect periods for which diaries and other archival data are present.

Throughout the 20th century, events were continuously and accurately monitored in the EPA and avalanche frequency increases to 0.34 events $yr^{-1}$ between 1901 and 2010 with 10-yr minima in 1965–1974 and 1989–1998 (one event each) and a 10-yr maximum between 1905 and 1914 (7 events). The type of avalanches (i.e. the quality of snow and the position of the sliding surface; Fig. 2a), date of occurrence (Fig. 2b, c) and runout elevation (Fig. 2 d) have been

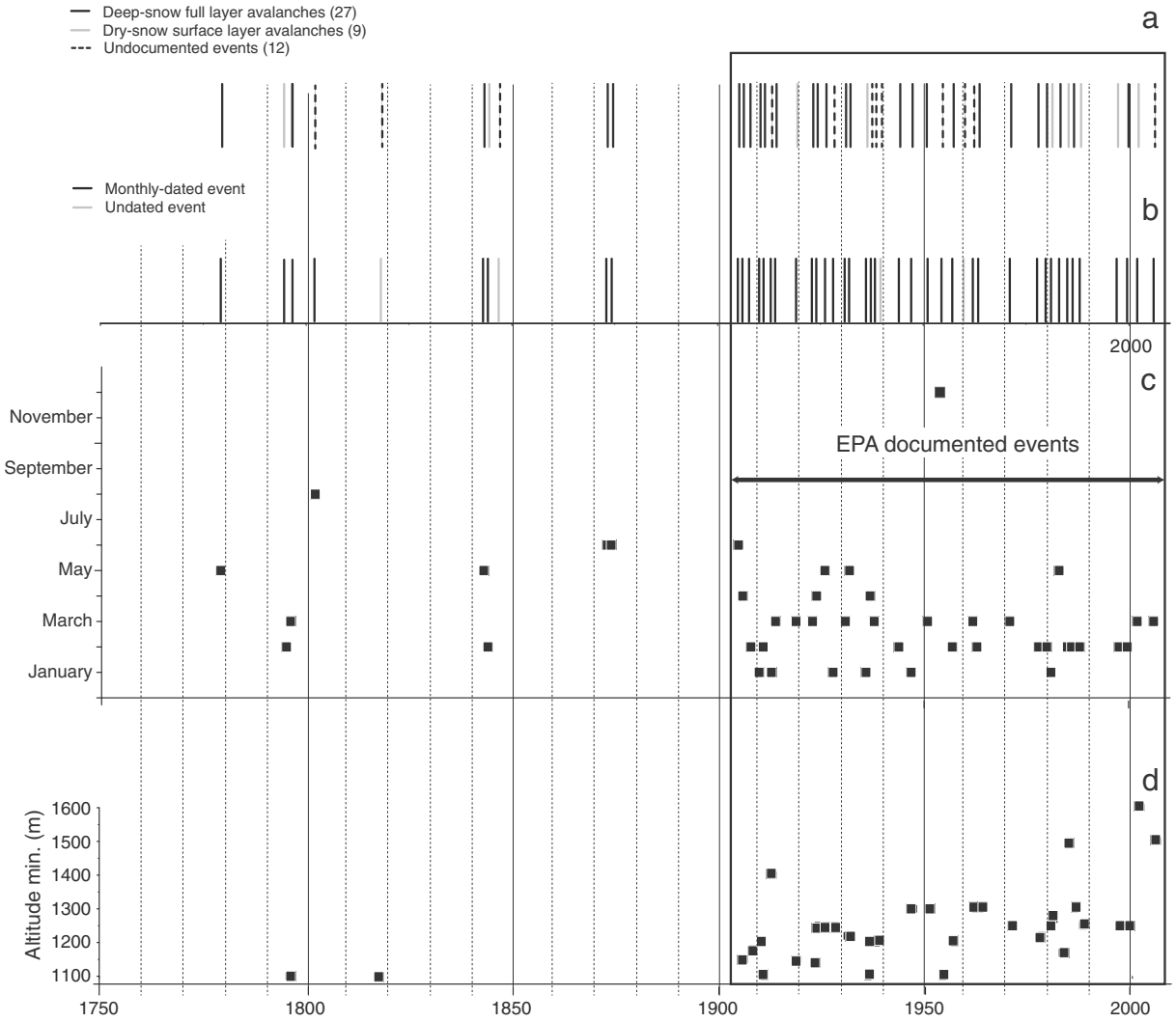


**Fig. 2.** Types (a), dates of occurrence (b, c) and runout elevations (d) of the documented avalanche events on the Pèlerins avalanche path.

described occasionally in historical archives (pre-20th century) and are more readily and systematically available in the EPA. Among the reconstructed events, a total of 27 events (56%) were classified full-depth avalanches in the EPA, 9 (19%) are described as surface layer avalanches and no classification exists for 12 events (25%; Fig. 2b). Among the 48 snow avalanches recorded, 31 occurred between December and March, 11 between April and July, and 6 were not precisely dated (Fig. 2c).

For the pre-20th century events, the runout elevation was rarely noted in historical documents (Fig. 2 d): For the 1779 avalanche, detailed writings allowed an estimation of the runout elevation to ~1200 m asl. In 1796 and 1818, runout elevations of avalanches were estimated to ~1100 m asl. For the period 1901–2010, runout elevations were documented for 32 snow avalanches and show an average of 1250 m asl with a maximum runout at 1100 m asl in 1911, 1936 and 1954 and a minimum at 1600 m asl in 2002. In addition, historical photographs, writings and technical reports enabled precise reconstruction of the slide extent of three major destructive events in 1924, 1931 and 1983 (Fig. 3a).

### 4.2. Types of growth disturbances related to snow avalanche activity

The 452 increment cores selected from the 209 trees permitted identification of 645 GD relating to past snow avalanche activity. Table 2 illustrates the nature of GD as well as their intensity. Abrupt growth reductions were the GD most frequently identified in the samples (356, 55%), followed by TRD (149, 23%), compression wood (80, 12%) and callus tissue (60, 9%). In total, 78% of the GD were rated severe, high-intensity disturbances (intensity classes 4 or 5). The oldest GD identified in the tree-ring series was dated to 1745. GD became more frequent after 1770, and nearly every year exhibited GD in a small number of trees (Fig. 4a, b). Some GD are clearly related to snow avalanche activity, but some are noise.

### 4.3. Determination of optimal thresholds for GD and It functions of sample size

Avalanche chronologies were successively computed using thresholds of 2–10 for GD and of 1–50% for *It*, for subsets of the samples randomly

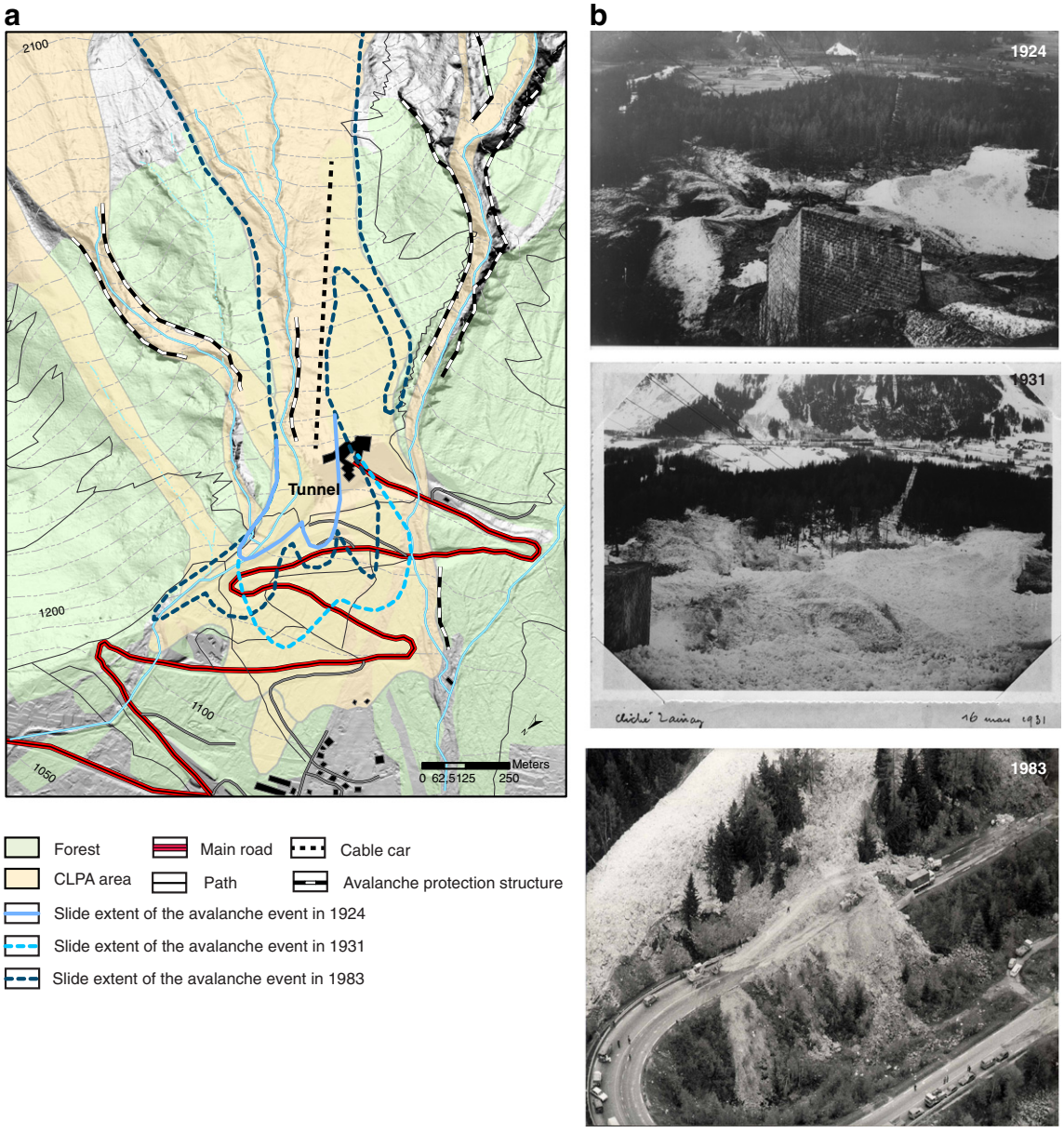


**Fig. 3.** Spatial extent (a) and historical photographs (b) of the major avalanche events in 1924, 1931 and 1983.

**Table 2**
Intensity reactions and types of growth disturbances (GD) assessed in the 209 trees selected for analysis.

| Intensity | Number | % | Type | Number | % |
|---|---|---|---|---|---|
| | | | Tangential rows of traumatic resin ducts | 149 | 23 |
| 1 | 8 | 1 | Compression wood | 80 | 12 |
| 2 | 81 | 13 | Callus tissue | 60 | 9 |
| 3 | 52 | 8 | Growth reduction | 356 | 55 |
| 4 | 153 | 24 | | | |
| 5 | 351 | 54 | | | |
| Total | 645 | 100 | | 645 | 100 |

extracted with sizes varying from 10 to 200 trees. The matrices presented in Fig. 5 illustrate the mean percentage of historical events known from archival records identified in the tree-ring records as well as the average number of events reconstructed in the tree-ring archives but absent from the EPA, after 1000 sampling iterations. For example, with 20 trees 27% of the documented events would have been reconstructed with dendrogeomorphic techniques. In this case, a low GD threshold (≥3 GD) can be used as it does not induce noise in the reconstruction (Fig. 5a). The percentage of events reconstructed with tree-ring data increases to 35% when 50 trees are used (Fig. 5b). The optimal thresholds for GD and *It* are 5 and 10%, respectively, in this case. If analysis is based on 100 trees, the mean percentage of reconstructed events after 1000 sampling iterations increases to 41%, but the cut-off for the minimum number of responding trees with GD needs to be fixed to 7 responders in this case to avoid the introduction of noise in the reconstruction (Fig. 5c). Finally, with 200 trees, the percentage of reconstructed events does not even increase (41%) with an optimal minimum of 9 GD corresponding to a minimal *It* of 4.5% (Fig. 5 d).

### 4.4. Reconstruction of avalanche events based on optimized thresholds

The reconstruction of past avalanche events was based on the GD and *It* thresholds presented in the previous paragraph and calibrated for the period where historical data from EPA was available (1905–2010). In total, GD did exceed the optimal thresholds for GD and *It* in 34 years after 1770 (Table 3); these years were considered avalanche years: 1771, 1774, 1779, 1791, 1795, 1796, 1807, 1836, 1843, 1851, 1866, 1869, 1874, 1878, 1880, 1885, 1897, 1906, 1911, 1916, 1923, 1924, 1928, 1931, 1932, 1937, 1947, 1951, 1960, 1962, 1971, 1981, 1983 and 1988. The years 1983 ($n=57$), 1931 ($n=40$), 1937 ($n=37$) and 1988 ($n=29$) are those exhibiting the largest number of trees with GD (Table 3, Fig. 4a). In a similar way, the largest frequency of appearance of trees with GD was measured in 1779 (37%), 1983 (27%), 1931 (24%) and 1937 (21%) (Table 3, Fig. 4b).

Considering the period since AD 1770, the overall return period (i.e. the average number of years between two events) is 7.1 yr and the mean decadal frequency is 1.4 events. This value slightly increases from 6.8 years for the period 1770–1904 to 7.5 years for the period 1905–2010. Maximum decadal frequencies (3 events) are observed in 1771–1780, 1791–1800, 1921–1930 and 1981–1990. Conversely, no event was reconstructed for the periods 1781–1790, 1811–1830 and since 1990.

The spatial distribution of trees affected by the same event was used to determine the minimum lateral reach (Fig. 6) and the minimum runout elevation (Table 3) of reconstructed avalanches. The mean runout elevation calculated for these events is 1490 m asl (±210 m) varying between 1775 m asl (1869) and 1184 m asl (1779). Large snow avalanches reached the current entrance of the Mont Blanc tunnel (1275 m) at least seven times in the past, namely in 1779 (Fig. 6a), 1906, 1931 (Fig. 6b), 1951, 1960, 1962, and 1983 (Fig. 6c). Based on the tree-ring record, it was also possible to reconstruct 10 minor events which stopped in the upper part of the path at a runout elevation >1700 m asl, namely in 1771, 1774, 1796, 1791, 1795, 1807, 1843, 1851, 1869, and 1981 (Table 3).

### 4.5. Comparison of historical archives with reconstructed events

For the period documented in the EPA, 16 out of the 37 avalanches (43%) are reconstructed using optimized thresholds for GD and *It*. Based on the tree-ring data, only one avalanche in 1916 was not listed in the EPA. Prior to 1905 (before the introduction of the EPA), the dendrogeomorphic reconstruction confirmed 5 events documented in historical archives (1779, 1795, 1796, 1843, and 1874) and added 13 undocumented events to the local database.

Although an optimized threshold was used for the identification of snow avalanches with tree-ring records, 21 of the 48 events documented since AD 1776 (43%) were identified as avalanches based on dendrogeomorphic criteria. From the 21 reconstructed events, based on archival information, 12 were full-depth avalanches, six were surface layer avalanches and three events could not be attributed to either of the avalanche types (Table 3). Runout elevations tend to be underestimated with dendrogeomorphic techniques by as little as 5 m (1937) to up to 464 m (1981; Table 3). On the other hand, it

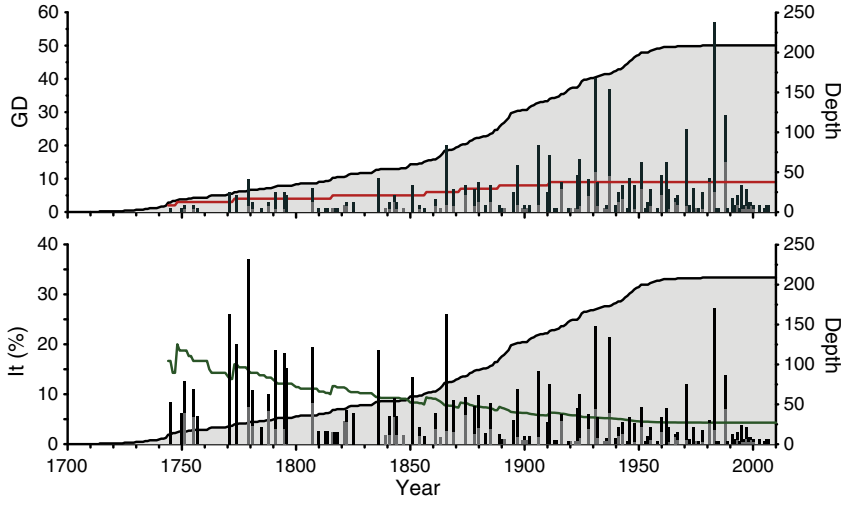


**Fig. 4.** Event-response histograms showing avalanche-induced growth responses from sampled trees. (a) Total number of growth disturbances (GD), and (b) percentage of trees responding to an event. Stacked bar graphs show the proportion of samples with high-intensity (4–5, dark shading) and low-intensity (1–3, light shading) GD. The red line demarcates (a) the thresholds used for GD. The green line in (b) demarcates the threshold used for index values (*It*). The grey area shows the total number of trees (*n*) alive each year.

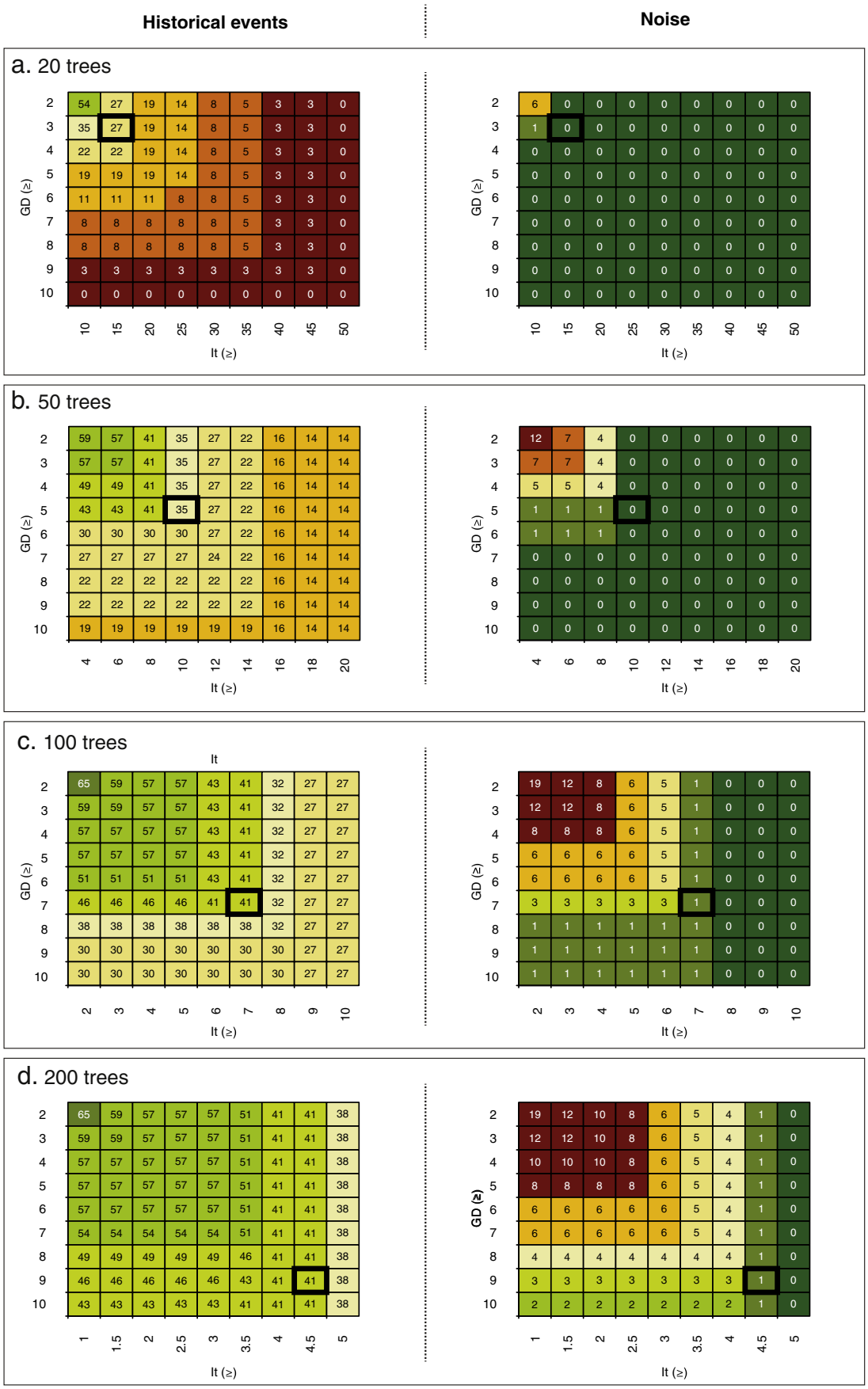


**Fig. 5.** Mean percentage of historical events (left panel) and mean number of undocumented events (noise, right panel) reconstructed from three-ring analysis, functions of the number of growth disturbances (GD) and index values (*It*). The mean of 1000 sampling iterations was calculated for subsets of (a) 20, (b) 50, (c) 100, and (d) 200 trees randomly extracted without replacement. The black boxes denote the optimal thresholds for GD and *It* that maximize the percentage of reconstructed events and minimize noise.

**Table 3**
Characteristics of the reconstructed events and comparison of minimal runout elevations computed from tree-ring analysis and from historical archives.

| Event year | GD | It | Type of avalanche | Runout altitude (m, tree-ring) | Runout altitude (m, historical archives) |
|---|---|---|---|---|---|
| 1771 | 6 | 26 | Undocumented event | 1758 | Undocumented |
| 1774 | 5 | 20 | Undocumented event | 1756 | Undocumented |
| 1779 | 10 | 37 | Deep-snow full layer | 1184 | <1200 (estimated) |
| 1791 | 6 | 19 | Undocumented event | 1740 | Undocumented |
| 1795 | 6 | 18 | Dry-snow surface layer | 1746 | Unknown |
| 1796 | 5 | 15 | Deep-snow full layer | 1731 | <1200 (estimated) |
| 1807 | 7 | 19 | Undocumented event | 1745 | Undocumented |
| 1836 | 10 | 19 | Undocumented event | 1370 | Undocumented |
| 1843 | 5 | 9 | Deep-snow full layer | 1754 | Unknown |
| 1851 | 8 | 13 | Undocumented event | 1757 | Undocumented |
| 1866 | 20 | 26 | Undocumented event | 1346 | Undocumented |
| 1869 | 5 | 6 | Undocumented event | 1775 | Undocumented |
| 1874 | 7 | 8 | Deep-snow full layer | 1608 | Unknown |
| 1878 | 6 | 7 | Undocumented event | 1602 | Undocumented |
| 1880 | 6 | 6 | Undocumented event | 1530 | Undocumented |
| 1885 | 8 | 8 | Undocumented event | 1637 | Undocumented |
| 1897 | 14 | 11 | Undocumented event | 1314 | Undocumented |
| 1906 | 20 | 15 | Deep-snow full layer | 1233 | 1150 (−83) |
| 1911 | 17 | 12 | Deep-snow full layer | 1470 | 1100 (−370) |
| 1916 | 9 | 6 | Undocumented event | 1640 | Undocumented |
| 1923 | 11 | 7 | Deep-snow full layer | 1461 | 1140 (−321) |
| 1924 | 14 | 9 | Deep-snow full layer | 1290 | 1250 (−40) |
| 1928 | 7 | 4 | Dry-snow surface layer | 1457 | 1250 (−207) |
| 1931 | 40 | 24 | Dry-snow surface layer | 1215 | 1220 (5) |
| 1932 | 9 | 5 | Unknown type | 1474 | Unknown |
| 1937 | 37 | 21 | Unknown type | 1322 | 1200 (−122) |
| 1947 | 10 | 5 | Deep-snow full layer | 1510 | 1300 (−210) |
| 1951 | 15 | 8 | Deep-snow full layer | 1219 | 1300 (81) |
| 1960 | 11 | 5 | Unknown type | 1241 | Unknown |
| 1962 | 15 | 7 | Dry-snow surface layer | 1220 | 1300 (80) |
| 1971 | 25 | 12 | Deep-snow full layer | 1282 | 1250(−32) |
| 1981 | 10 | 5 | Dry-snow surface layer | 1734 | 1270 (−464) |
| 1983 | 57 | 27 | Deep-snow full layer | 1190 | 1170 (−20) |
| 1988 | 29 | 14 | Dry-snow surface layer | 1411 | 1250 (−161) |

can also be seen from Fig. 6 that reconstructed avalanche events frequently exceeded the lateral limits of the CLPA map, particularly above 1600 m asl. Even for the most accurately documented events of 1924, 1931, and 1983 (Fig. 6), discrepancies exist between the lateral spread as reconstructed with dendrogeomorphic techniques and results obtained from contemporary photographs and technical reports.

## 5. Discussion

### 5.1. Optimal sample size

In his seminal paper, Shroder (1978) emphasizes that sample size may be a moot question unless site selection ensures that trees are responding to the process under investigation. We agree that site selection is important (Stoffel and Bollschweiler, 2008), but consider that Butler's (1987) questions of how many trees should be sampled and how many of the sampled trees must illustrate tree-ring responses before the inference of an event can be accepted are at least as critical as site selection.

The study we report here is the first to quantitatively address and calibrate optimal thresholds for both sample size and growth disturbance (GD, *It*) on a forested avalanche path where events have been monitored accurately and continuously over the entire 20th century. For the purpose of calibrating optimal index values, avalanche chronologies were successively computed for subsets of the entire sample (209 trees) and subset sample sizes were varied between 10 and 200 trees. Results demonstrate very clearly that the percentage of known events (i.e. those noted in the EPA) to be replicated with tree-ring records increases with sample size to an optimum of ~100 disturbed trees and remains relatively stable above this value. Interestingly, this threshold clearly exceeds the sample size reported in numerous studies published in the past (Table 1). Although it is clearly not our purpose to reject studies which have been based on a smaller sample sizes, we realize that discrete processes such as snow avalanches are more accurately reconstructed with a larger sample size (Butler, 1987). The apparent existence of a plateau in reconstruction above ~100 trees may also be helpful for the design of sampling campaigns at new sites and can help to more accurately plan fieldwork (in terms of time and budget). This sample size should be adjusted according to the morphology of the path, the stand and the GD densities and the response of tree species against avalanche impacts.

### 5.2. Avalanche reconstruction and minimal index values

Previous studies used different minimal indices (*It*) values ranging from 10% (e.g., Dubé et al., 2004) to 40% (e.g., Butler and Malanson, 1985). In our study, a large set of archival records was available to calibrate GD in tree-ring series with documented snow avalanche events for the entire 20th century. The calibration for the documented period demonstrated quite clearly that a reconstruction based on dendrogeomorphic techniques is optimized if the thresholds for *It* and GD are adjusted to sample size. When sample size is still small (<20 trees), a 10% *It* infers an avalanche event on the basis of two GD and therefore induces a lot of noise (6 undocumented events) into the reconstruction. On the other extreme, an *It* threshold of 40% appears to be much too stringent even for a small sample size, and only 5% (2 out of 37 events) of the events recorded in archival records would have been recognized in the tree-ring series.

Based on these considerations and on the results presented in Fig. 5, our study suggests that an optimal index value of ~15% should be used with a small sample size to capture a maximum of snow avalanches without introducing noise. With a very large sample size (>200 trees), the optimal *It* can be reduced to 5% without introducing significant noise to the reconstruction. With an *It* of 5%, the only event trespassing the threshold without being noted in the archives occurred in 1916, i.e. during World War 1 for which the lacunary character of the database has been described in the past (Ancey, 2004).

### 5.3. Temporal accuracy of the reconstruction

When optimized thresholds are used for GD and *It*, 34 events can be reconstructed for the Pèlerins avalanche track for the last 239 yr (1771–2010). The reconstruction was successful overall as (i) it complemented the existing snow avalanche chronology and (ii) extended it back to 1771, (iii) added one event which was not previously known for the period with EPA records (1905–2010) and 12 for the time before 1905. From the 37 snow avalanches recorded in the EPA, 16 could be confirmed with dendrogeomorphic techniques. In addition, five of the reconstructed pre-20th century snow avalanches were confirmed via other historical sources. The optimized thresholds, calibrated for the period documented by the EPA, minimized the likelihood that GD resulting from non-avalanche events were included in the chronology (Reardon et al., 2008). The thresholds also facilitated rejection of GD related to other geomorphic processes such as snow creep or rockfall which have been shown to affect a rather limited number of trees per event (Stoffel and Perret, 2006). For years with threshold exceedances, the presence of clear and strong signs of physical impact (injuries and adjacent callus tissue and/or other severe GD, i.e. intensity 4 and 5 reactions) was used as a further criterion for a doubtless dating of snow avalanche events.

However, the comparison between historical archives and tree-ring records at Les Pèlerins suggests that the dendrogeomorphic reconstruction

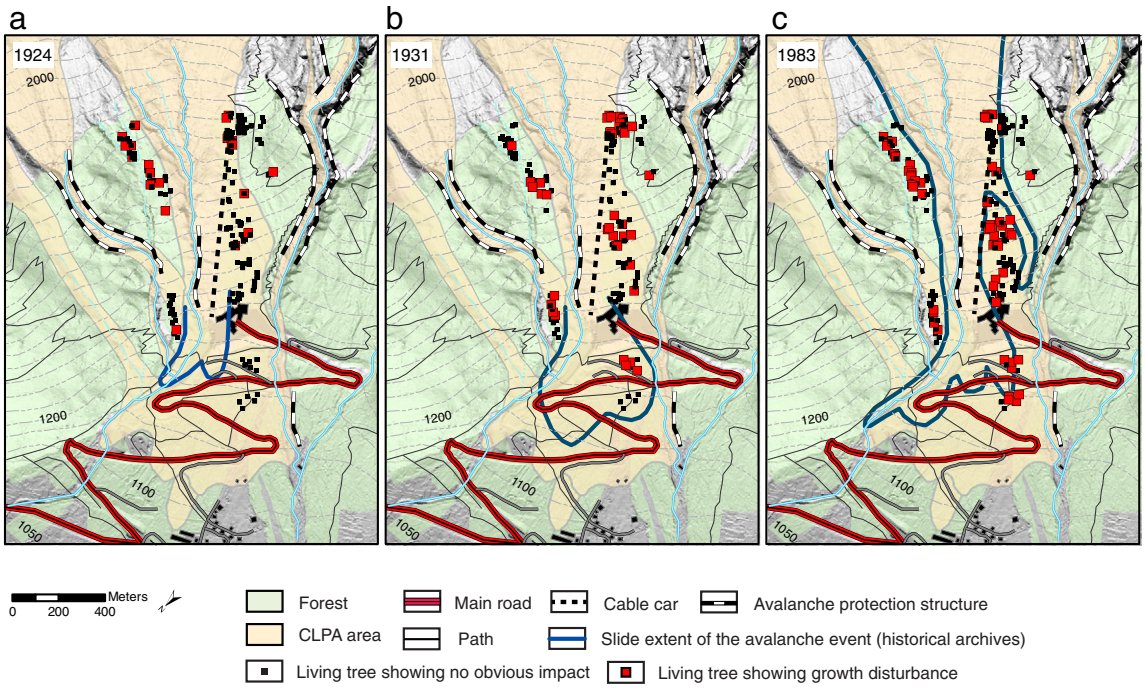


**Fig. 6.** Reconstructed minimum avalanche extent in the runout zone for the events of (a) 1924, (b) 1931, and (c) 1983 and comparison with historical limits derived from technical reports and photographs. Maps show living trees and all trees showing an event-response for the year of the avalanche.

underestimates years with natural avalanche activity by roughly 60%. This proportion slightly exceeds the 50% value of unreconstructed events reported by Corona et al. (2010) in the Oisans massif (French Alps). In any case, the number of reconstructed snow avalanches has to be seen as a minimum frequency of natural avalanches, mainly for the following reasons: Avalanches have to be of sufficient magnitude to have significant impacts on trees. Critical snow pressures for stem breakage of trees have been deduced mainly from theoretical models and observational studies (Bebi et al., 2009; Bartelt and Stöckli, 2001) and have shown to depend on stem diameter and avalanche type. For flowing avalanches (characterized by a high snow density at the bottom), it can be expected that only the events with typical masses $>100\ m^3$, a path length >100 m and an impact pressure >50 kPa – i.e. destructive class 2 or larger according to McClung and Schaerer (1993) or Reardon et al. (2008) – will emerge from the tree-ring record. For powder snow avalanches, critical pressures for an event to be identified in a tree-ring record are lower (3–5 kPa) as not only the stem but also the crown of a tree is exposed to avalanche pressure (Bebi et al., 2009).

Another reason for differences in ecosystem responses of individual trees to snow avalanches are related to tree size and flexibility (Bebi et al., 2009; Kajimoto et al., 2004). A tree flexible enough to be deflected may remain largely undamaged by the avalanche. Small *P. abies*, *L. decidua* or Cembran pine (*Pinus cembra* L.) trees with heights <5 m and diameters <15–20 cm have been shown to tolerate snow pressure by bending and leaning in the snowpack (Bebi et al., 2009).

While the methodology presented in this study minimizes the risk of including non-avalanche events in the chronology, it most likely also creates a bias towards larger avalanches, as smaller snow avalanches or events limited to the non-forested parts of the avalanche talus cone cannot be identified by means of tree-ring analysis. This fact is for example supported by archival data for the events of 1913, 1951, 1985, 1986, or 2002, where the EPA notes the presence of snow avalanches with limited extension. These events do not therefore appear in the tree-ring based reconstruction, since they did not affect forested areas or the number of trees sampled in the area affected was small and therefore the number of GD observed in the tree-ring series did not exceed the threshold. In addition, major avalanches may remove or blur the evidence of previous or subsequent events in case large parts of the forest are destroyed (e.g., Bryant et al., 1989; Carrara, 1979) or disturb tree growth in such a way that younger events cannot be identified in the tree-ring record (Kogelnig-Mayer et al., 2011). For example, we find a large number of trees showing GD as a result of the avalanche activity of 1779, 1911, and 1937, but fail to identify the events between 1780 and 1790 or for consecutive years with avalanche activity noted in the EPA (e.g., 1913, 1914 or 1938, 1939).

### 5.4. Spatial accuracy of the reconstruction

The spatial reconstruction of snow avalanches using tree-ring records matches well with archival data and technical reports of the large events in 1924, 1931, and 1983, especially concerning the runout elevation. In contrast, the dendrogeomorphic reconstruction largely underestimates runout elevations for the events in 1796, 1911, 1923, 1928, 1947, 1981, and 1988. Underestimation might be related to (i) the modification of path geometry (steepness, curvature) by the geomorphic effect of the avalanches in the runout zone below 1300 m asl. These modifications may have induced rapid avalanche deceleration (McClung, 1990; McClung and Schaerer, 1985) and snow pressures insufficient to damage trees during some of the events listed above; (ii) observation inaccuracies in the EPA typically ranging from 25 m for the older to 10 m for the more recent events (Ancey, 2004). Indeed, for safety reasons, runout elevations noted in the EPA are not measured *in situ* but estimated from observation points and manually plotted on a map. For extreme events involving very dry, non cohesive snow and/or a powder cloud, the point of the farthest reach is sometimes very difficult to be located because of the absence of clearly visible deposits (Eckert et al., 2010).

Large discrepancies are also reported between the lateral limits reconstructed with dendrogeomorphic techniques and the data reported in technical reports and the CLPA. For several events, we identify trees with avalanche damage some 50–100 m outside of the CLPA limits, especially above 1600 m asl (Fig. 6). Uncertainties of CLPA boundaries have in fact been estimated to >50 m (Ancey, 2006; Bonnefoy et al., 2010), albeit, theoretically, the CLPA should contain the maximum boundaries of historically known avalanches.

Yet, the CLPA map is drawn for large areas (scale 1:25,000) and compiled from various sources (historical archives and interviews, field observations and photo interpretation) with often no or only very limited data on the lateral spread of avalanches (Bonnefoy et al., 2010). Furthermore, such discrepancies may be related to the lateral extent of powder snow avalanches that is very difficult to evaluate for an observer.

## 6. Conclusions

Evaluating the potential of tree-ring analysis on an extensively and accurately documented (1905–2010) avalanche path located in the Chamonix valley (French Alps) reveals (i) that ~100 trees are needed to obtain the best match between reconstruction and historical archives while minimizing the inclusion of noise in the dendrogeomorphic record. This threshold is not absolute but suggests that chronologies for geographically discrete processes, such as avalanches, should aim for a high sample size; (ii) increasing GD thresholds adjusted to sample size should be preferred to fixed values used in previous work; (iii) tree-ring analysis proves to be a valuable source of information to reconstruct past avalanche events and to add substantially to the historic record for this area, particularly for the undocumented period (1770–1904). Yet, one must keep in mind that the reconstruction represents a minimum frequency for past avalanche events as ~40% of all documented events were deciphered with dendrogeomorphic techniques; (iv) because of increased human activity in mountain areas, the identification of area endangered is of paramount importance. For this purpose, dendrogeomorphic should be used systematically where woody vegetation is available to add evidence on the runout distance of large events and to determine the lateral spread of past avalanches. It should though represent a valuable tool for avalanche hazard mapping where other sources often fail to produce conclusive results.

## Acknowledgements

This research has been supported by the Cemagref, by the PARAMOUNT program, 'ImProved Accessibility, Reliability and security of Alpine transport infrastructure related to MOUNTainous hazards in a changing climate', funded by the Alpine Space Programme, European Territorial Cooperation, 2007–2013 and the DENDROGLISS program, funded by the MAIF foundation. M.S. acknowledges support from the Era.Net CIRCLE Mountain project "ARNICA". The authors would like address warm thanks to Severine Finet for her essential contribution on developing routines.

## References

Alestalo, J., 1971. Dendrochronological interpretation of geomorphic processes. Fennia 105, 1–139.
Ancey, C., 2004. Computing extreme avalanches. Cold Regions Science and Technology 39, 161–180.
Ancey, C., 2006. Dynamique des avalanches. Presses polytechniques et universitaires Romandes, Cemagref. Lausanne, Antony (France).
Bartelt, P., Stöckli, V., 2001. The influence of tree and branch fracture, overturning and debris entrainment on snow avalanche flow. Annals of Glaciology 32, 209–216.
Bebi, P., Kulakowski, D., Rixen, C., 2009. Snow avalanche disturbances in forest ecosystems—state of research and implications for management. Forest Ecology and Management 257, 1883–1892.
Bollschweiler, M., Stoffel, M., Schläppy, R., 2011. Debris-flood reconstruction in a pre-alpine catch-ment in Switzerland based on tree-ring records of coniferous and broadleaved trees. Geografiska Annaler: Series A, Physical Geography 93, 1–15.
Bonnefoy, M., Escande, S., Cabos, S., Gaucher, R., Pasquier, X., Tacnet, J., 2010. Localization map of avalanche phenomena (CLPA) and collection of eye witness accounts: field investigation method, biases, alternatives and limits, data quality. International Snow Science Workshop, October 17–22, Squaw Valley, CA.
Bryant, C.L., Butler, D.R., Vitek, J.D., 1989. A statistical analysis of tree-ring dating in conjunction with snow avalanches: comparison of on-path versus off-path responses. Environmental Geology and Water Sciences 14, 53–59.
Butler, D.R., 1987. Teaching general principles and applications of dendrogeomorphology. Journal of Geological Education 35, 64–70.
Butler, D.R., Malanson, G.P., 1985. A history of high-magnitude snow avalanches, Southern glacier national park, Montana, U.S.A. Mountain Research and Development 5, 175–182.
Butler, D.R., Sawyer, C.F., 2008. Dendrogeomorphology and high-magnitude snow avalanches: a review and case study. Natural Hazards and Earth System Science 8, 303–309.
Butler, D., Malanson, G., Oelfke, J., 1987. Tree-ring analysis and natural hazard chronologies: minimum sample sizes and index values. The Professional Geographer 39, 41–47.
Cachat, J., 2000. Les carnets de Cachat le Géant: mémoires de Jean-Michel Cachat dit "Le Géant", guide de monsieur de Saussure, paysan de la vallée de Chamonix. La Fontaine de Siloé, Montmélian.
Carrara, P.E., 1979. The determination of snow avalanche frequency through tree-ring analysis and historical records at Ophir, Colorado. Geological Society of America Bulletin 90, 773.
Casteller, A., Stöckli, V., Villalba, R., Mayer, A.C., 2007. An evaluation of dendroecological indicators of snow avalanches in the Swiss Alps. Arctic, Antarctic, and Alpine Research 39, 218–228.
Casteller, A., Villalba, R., Araneo, D., Stöckli, V., 2011. Reconstructing temporal patterns of snow avalanches at Lago del Desierto, Southern Patagonian Andes. Cold Regions Science and Technology 67, 68–78.
Chaubet, D., 2011. Les cahiers de l'oncle ambroise, un chamoniard "ordinaire" (1867–1942). Célèbres ou obscurs. Hommes et femmes dans leurs territoires et leur histoire, Editions du CTHS, Bordeaux, pp. 259–267.
Corona, C., Rovéra, G., Lopez Saez, J., Stoffel, M., Perfettini, P., 2010. Spatio-temporal reconstruction of snow avalanche activity using tree rings: Pierres Jean Jeanne avalanche talus, Massif de l'Oisans, France. Catena 83, 107–118.
Deline, P., 2009. Interactions between rock avalanches and glaciers in the Mont Blanc massif during the late Holocene. Quaternary Science Reviews 28, 1070–1083.
Dubé, S., Filion, L., Hétu, B., 2004. Tree-ring reconstruction of high-magnitude snow avalanches in the Northern Gaspé Peninsula, Québec, Canada. Arctic, Antarctic, and Alpine Research 36, 555–564.
Eckert, N., Parent, E., Kies, R., Baya, H., 2009. A spatio-temporal modelling framework for assessing the fluctuations of avalanche occurrence resulting from climate change: application to 60 years of data in the northern French Alps. Climatic Change 101, 515–553.
Eckert, N., Baya, H., Deschatres, M., 2010. Assessing the response of snow avalanche runout altitudes to climate fluctuations using hierarchical modeling: application to 61 winters of data in France. Journal of Climate 23, 3157–3180.
ETNA, C., 2000. Commune de Chamonix Mont Blanc, projet de centre de secours principal près dès Pèlerins, étude du risque d'avalanche. Technical Report. Cemagref, F. Rapin (coord.).
Germain, D., Filion, L., Hétu, B., 2009. Snow avalanche regime and climatic conditions in the Chic-Choc Range, eastern Canada. Climatic Change 92, 141–167.
Hebertson, E., Jenkins, M.J., 2003. Historic climate factors associated with major avalanche years on the Wasatch Plateau, Utah. Cold Regions Science and Technology 37, 315–332.
Holmes, R.L., 1983. Computer-assisted quality control in tree-ring dating and measurement. Tree-Ring Bulletin 43, 69–75.
Jamard, A., Garcia, S., Bélanger, L., 2002. L'enquête permanente sur les Avalanches (EPA). Statistique descriptive générale des événements et des sites. DESS Ingéniérie Mathématique. Université Joseph Fourier, Grenoble, France.
Johnson, E.A., 1987. The relative importance of snow avalanche disturbance and thinning on canopy plant populations. Ecology 68, 43–53.
Kajimoto, T., Daimaru, H., Okamoto, T., Otani, T., Onodera, H., 2004. Effects of snow avalanche disturbance on regeneration of subalpine *Abies mariesii* forest, Northern Japan. Arctic, Antarctic, and Alpine Research 36, 436–445.
Kogelnig-Mayer, B., Stoffel, M., Bollschweiler, M., Hübl, J., Rudolf-Miklau, F., 2011. Possibilities and limitations of dendrogeomorphic time-series reconstructions on sites influenced by debris flows and frequent snow avalanche activity. Arctic, Antarctic and Alpine Research, 43, 649–658.
Lagotala, H., 1927. Etude de l'avalanche des Pèlerins (Chamonix). Technical report. Société Générale d'Imprimerie, Genève.
Lambert, R., 2009. Cartozonage: de la carte au zonage du risque avalanche. Neige et glace de montagne: reconstitution, dynamiques, pratique. Edytem 8, 233–237.
Leone, S., 2006. Les Populations de haute montagne face aux contraintes naturelles. Les vallées de Chamonix et Vallorcine (1730–1914). Ph.D. thesis. Université Pierre Mendès France. Grenoble, France.
Luckman, B.H., 2010. Dendrogeomorphology and snow avalanche research. In: Stoffel, M., Bollschweiler, M., Butler, D.R., Luckman, B.H. (Eds.), Tree rings and natural hazards. A state-of-the-art. Springer, Dordrecht, Heidelberg, London, New York, pp. 27–34.
Malanson, G.P., Butler, D.R., 1984. Transverse pattern of vegetation on avalanche paths in the northern Rocky Mountains, Montana. Great Basin Naturalist 44, 454–458.
McClung, D., 1990. A model for scaling avalanche speeds. Annals of Glaciology 36, 188–198.
McClung, D., Schaerer, P., 1985. Characteristics of flowing snow and avalanche impact pressures. Annals of Glaciology 6, 9–14.
McClung, D., Schaerer, P., 1993. The avalanche handbook. Mountaineers, Seattle.
Muntán, E., Garcia, C., Oller, P., Marti, G., Garcia, A., Gutierrez, E., 2009. Reconstructing snow avalanches in the Southeastern Pyrenees. Natural Hazards and Earth System Science 9, 1599–1612.
Ozenda, P., 1985. La végétation de la chaîne alpine dans l'espace montagnard européen. Masson, Paris.
Potter, N., 1969. Tree-ring dating of snow avalanche tracks and the geomorphic activity of avalanches, northern Absaroka Mountains, Wyoming, Boulder, CO. Geological Society of America Special Paper 123, 141–165.
Reardon, B.A., Pederson, G.T., Caruso, C.J., Fagre, D.B., 2008. Spatial reconstructions and comparisons of historic snow avalanche frequency and extent using tree rings in Glacier National Park, Montana, U.S.A. Arctic, Antarctic, and Alpine Research 40, 148–160.

Rinntech, 2009. http://www.rinntech.com/content/blogcategory/2/28/lang,english/2009.
Schaerer, P., 1972. Terrain and vegetation of snow avalanche sites at Rogers Pass, British Columbia. In: Slaymaker, O., McPherson, H.J. (Eds.), Mountain Geomorphology: Geomorphological Processes in the Canadian Cordillera. Tantalus Research Ltd. Edition, Vancouver B.C., pp. 215–222.
Schneuwly, D.M., Stoffel, M., Bollschweiler, M., 2008. Formation and spread of callus tissue and tangential rows of resin ducts in *Larix decidua* and *Picea abies* following rockfall impacts. Tree Physiology 29, 281–289.
Shroder, J., 1978. Dendrogeomorphological analysis of mass movement on Table Cliffs Plateau, Utah. Quaternary Research 9, 168–185.
Shroder, J., 1980. Dendrogeomorphology; review and new dating techniques of tree-ring dating. Progress in Physical Geography 161–188.
Stoffel, M., Bollschweiler, M., 2008. Tree-ring analysis in natural hazards research – an overview. Natural Hazards and Earth System Science 8, 187–202.
Stoffel, M., Bollschweiler, M., 2009. What tree rings can tell about earth-surface processes. Teaching the principles of dendrogeomorphology. Geography Compass 3, 1013–1037.
Stoffel, M., Hitz, O.M., 2008. Snow avalanche and rockfall impacts leave different anatomical signatures in tree rings of *Larix decidua*. Tree Physiology 28 (11), 1713–1720.
Stoffel, M., Perret, S., 2006. Reconstructing past rockfall activity with tree rings: some methodological considerations. Dendrochronologia 24, 1–15.
Stoffel, M., Bollschweiler, M., Hassler, G., 2006. Differentiating past events on a cone influenced by debris-flow and snow avalanche activity – a dendrogeomorphological approach. Earth Surface Processes and Landforms 31, 1424–1437.
Stoffel, M., Bollschweiler, M., Butler, D.R., Luckman, B., 2010a. Tree rings and natural hazards: A state-of-the-art. Springer, Dordrecht; New York.
Stoffel, M., Bollschweiler, M., Widmer, S., Sorg, A., 2010b. Spatio-temporal variability in debris¬flow activity: a tree-ring study at Geisstriftbach (Swiss Alps) extending back to AD 1736. Swiss Journal of Geosciences 103, 283–292.
Timell, T., 1986. Compression wood in gymnosperms. Springer, Berlin.
Zumbühl, H., Steiner, D., Nussbaumer, S., 2008. 19th century glacier representations and fluctuations in the central and western European Alps: an interdisciplinary approach. Global and Planetary Change 60, 42–57.